ACCSCIENCE PUBLISHING

International Journal of Bioprinting

RESEARCH ARTICLE

Light-based and cost-effective bioprinting of musculoskeletal GelMA constructs enriched with mesoporous bioactive glass nanoparticles

Supplementary file

1. Introduction

In this section, we provide supplementary characterization data for mesoporous bioactive glass nanoparticles (MBGNs) and gelatin methacryloyl enriched with MBGNs (GelMA-MBGNs composites). These supplementary analyses aim to further elucidate the structural and physicochemical properties of MBGNs and their composites with GelMA, providing complementary information of their role in our bioprinted constructs.

2. Methods

2.1. Scanning electron microscopy (SEM)

Figure S1A depicts visualized MGBNs using a scanning electron microscope (EVO/MA25, Zeiss, Oberkochen, Germany) operating in high vacuum mode. For this, MBGNs were dried into a coating pin using isopropyl alcohol as the solvent. Once the nanoparticles were evenly dispersed on the coating pin, they were allowed to dry completely. Subsequently, a thin layer of gold was sputter-coated onto the dried nanoparticles to enhance their surface conductivity and improve imaging quality during SEM analysis. Image analysis was performed using ImageJ software to obtain the nanoparticle diameter distribution.

2.2. X-ray diffraction (XRD)

GelMA hydrogel (control), GelMA enriched with MBGNs, and the MBGNs were subjected to XRD analysis using a Rikagu Miniflex 600 (Rikagu Corporation, Tokyo, Japan), operated with Cu-Kα as a radiation source, a current of 15 mA, and a voltage of 40 kV. Hydrogel samples were freeze-dried and cut into small sizes for XRD analysis.

2.3. Fourier-transform infrared spectrometer (FTIR)

GelMA hydrogel (control), GelMA enriched with MBGNs, and MBGNs were analyzed using a FTIR spectrometer Spectrum-400 (Perkin Elmer Waltham, MA, USA) at a frequency range of 4000–400 cm−1. SpectrumTM software from Perkin–Elmer was used for analysis of spectra, and the spectra were normalized and the baseline was corrected. Hydrogel samples were freeze-dried and cut into small sizes for FTIR analysis.

3. Results and discussions

Figure S1A shows an SEM image of MBGNs. The SEM image reveals that the MBGNs exhibit a round morphology and appear to be clustered. Notably, the size of these particles is 159 ± 29 nm (see Figure S1B), which closely corresponds to the size reported in the literature.[1]

The XRD analysis results for the hydrogels are illustrated in Figure S2. The absence of significant peaks in the diffraction patterns of freeze-dried hydrogels corroborates the anticipated amorphous structure.[2] Conversely, MBGNs exhibit an amorphous silicate state, evidenced by a broad band at $2\theta = 23°$.[3] Notably, there are no pronounced peaks indicative of the crystallized structures commonly seen in glassy materials.[4]

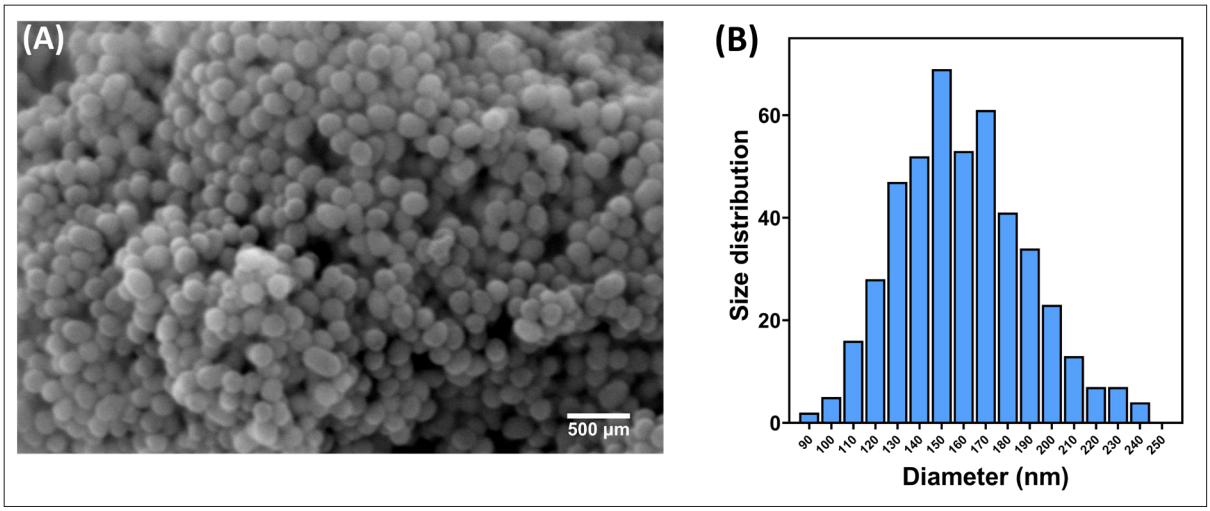

Figure S1. Scanning electron microscopy (SEM)-based analysis and size characterization of mesoporous bioactive glass nanoparticles (MBGNs). (A) SEM image. (B) Bar chart showing the size distribution of nanoparticles based on diameter.

Figure S3 corresponds to the FTIR analysis. The black spectrum represents the control GelMA without MBGNs, while the blue spectrum represents GelMA with MBGNs. Both spectra exhibit characteristic bands associated with hydrogels: the bands located at approximately 1540 and 1634 cm^{-1} are attributed to the –NH amino group. These bands are indicative of the bending and symmetric stretching vibrations of the –NH amino group. The band at approximately 3306 cm^{-1} is associated with the –OH group. This band is typically broad due to the hydrogen bonding of the –OH groups between molecules. The bands at approximately 1425 and 1450 cm^{-1} are assigned to the carbonate group. The presence of these bands in the spectra confirms the incorporation of MBGNs into the GelMA

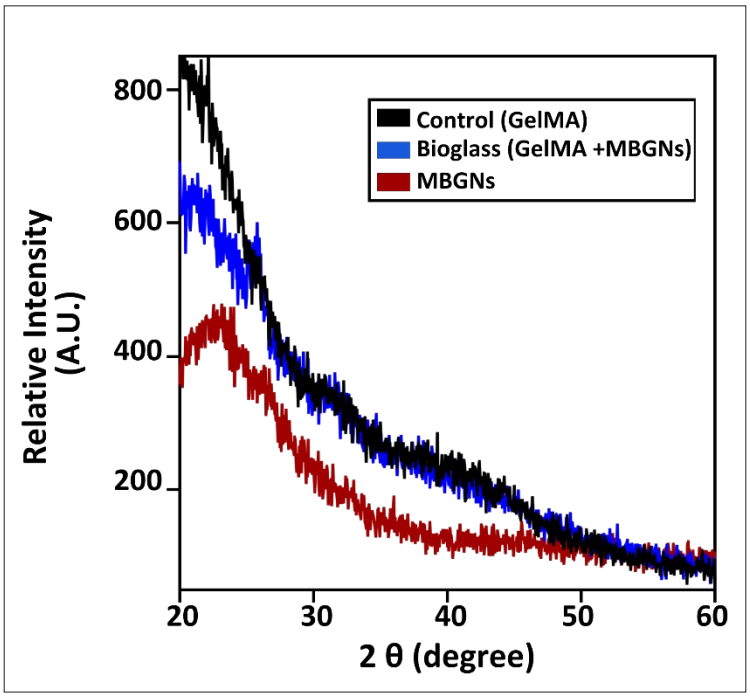

Figure S2. X-ray diffraction (XRD) spectra of various samples. The spectra reveal distinct patterns for each sample suggesting their respective amorphous structure.

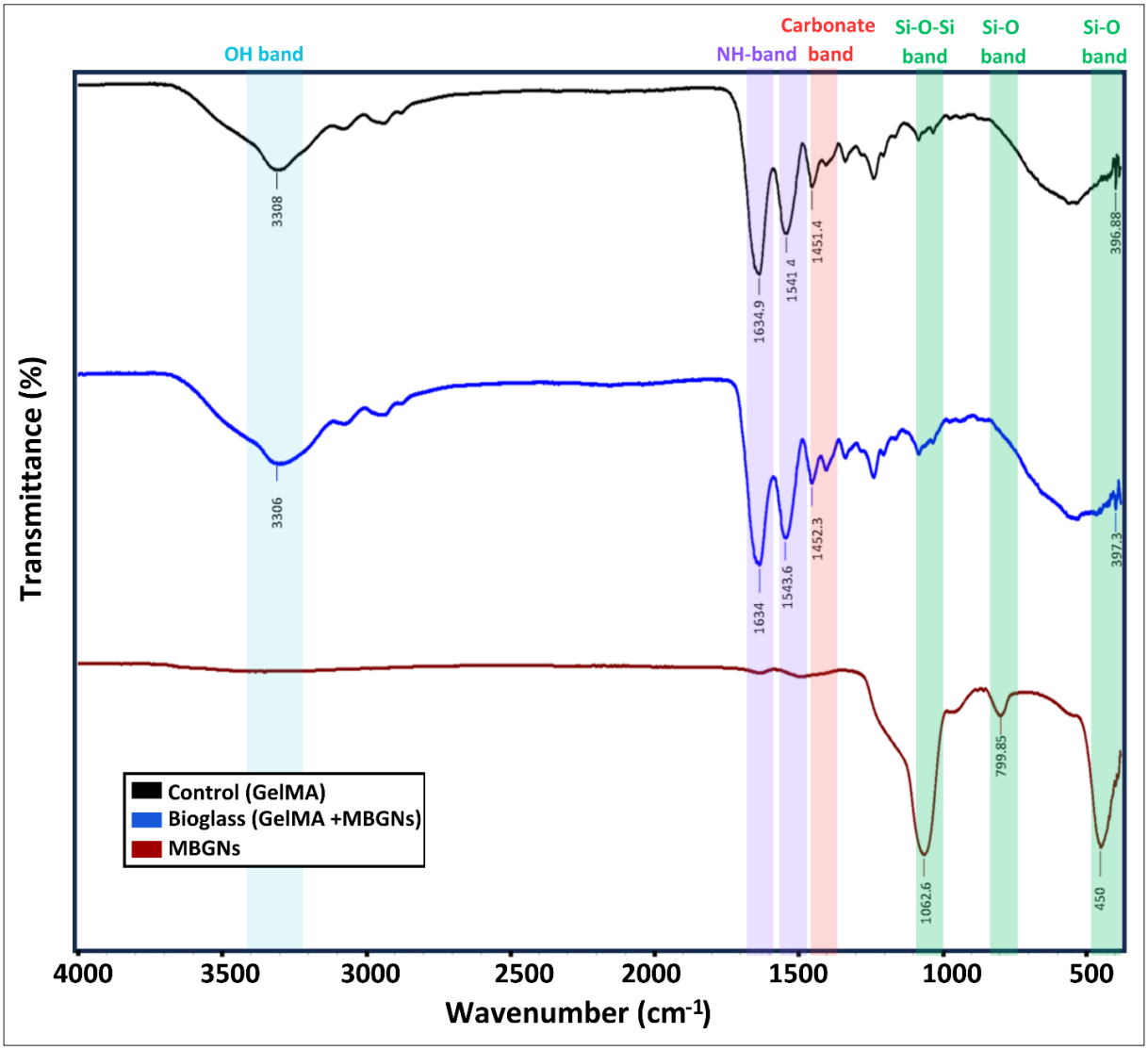

Figure S3. FTIR spectra of different samples. The spectra demonstrate the distinct vibrational frequencies of each sample.

without altering its fundamental chemical structure. The red spectra representing the MBGNs shows the presence of two bands at approximately 450 and 799 cm^{-1}, which are attributed to the bending and symmetric stretching vibrations of Si–O–Si, respectively. Furthermore, the band observed at around 1062 cm^{-1} is indicative of the vibrations associated with Si–O–Si bridging bonds.[1,5–7]

References

1. Zheng K, Kang J, Rutkowski B, et al. Toward highly dispersed mesoporous bioactive glass nanoparticles with high Cu concentration using Cu/ascorbic acid complex as precursor. *Front Chem*. 2019;7:497.
doi: 10.3389/fchem.2019.00497

2. Choi JB, Kim YK, Byeon SM, et al. Fabrication and characterization of biodegradable gelatin methacrylate/biphasic calcium phosphate composite hydrogel for bone tissue engineering. *Nanomater Basel Switz*. 2021;11(3):617.
doi: 10.3390/nano11030617

3. Bari A, Bloise N, Fiorilli S, et al. Copper-containing mesoporous bioactive glass nanoparticles as multifunctional agent for bone regeneration. *Acta Biomater*. 2017;55:493-504.
doi: 10.1016/j.actbio.2017.04.012

4. Öksüz K. Effect of composition and sintering temperature on the structure and properties of porous bioactive glass scaffolds. *Chiang Mai J Sci*. 2019;46:568-578.

5. Sitarz M, Handke M, Fojud Z, Jurga S. Spectroscopic studies of glassy phospho-silicate materials. *J Mol Struct*. 2005;744:621-626.
doi: 10.1016/j.molstruc.2004.12.050

6. Aguiar H, Serra J, González P, León B. Structural study of sol–gel silicate glasses by IR and Raman spectroscopies. *J Non-Cryst Solids*. 2009;355(8):475-480.
doi: 10.1016/j.jnoncrysol.2009.01.010

7. Wajda A, Sitarz M. Structural and microstructural comparison of bioactive melt-derived and gel-derived glasses from CaO-SiO2 binary system. *Ceram Int*. 2018;44(8): 8856-8863.
doi: 10.1016/j.ceramint.2018.02.070